

# Enhancement factor distribution around a single SERS Hot-spot and its relation to Single Molecule detection

E. C. Le Ru,\* P. G. Etchegoin,<sup>†</sup> and M. Meyer

*The MacDiarmid Institute for Advanced Materials and Nanotechnology, School of Chemical and Physical Sciences, Victoria University of Wellington, PO Box 600, Wellington, New Zealand*

(Dated: February 2, 2008)

We provide the theoretical framework to understand the phenomenology and statistics of single-molecule (SM) signals arising in Surface-Enhanced Raman Scattering (SERS) under the presence of so-called electromagnetic hot-spots (HS's). We show that most characteristics of the SM-SERS phenomenon can be tracked down to the presence of tail-like (power law) distribution of enhancements and we propose a specific model for it. We analyze, in the light of this, the phenomenology of SM-SERS and show how the different experimental manifestations of the effect reported in the literature can be analyzed and understood under a unified “universal” framework with a minimum set of parameters.

## I. INTRODUCTION

The possible detection of a Single Molecules (SM) by Surface Enhanced Raman Scattering (SERS) has played an important role in reviving the interest in SERS.<sup>1,2</sup> However, most of the evidence originally put forward in favor of SM-SERS were indirect. For each piece of evidence, one could usually find an alternative explanation that did not require SM-SERS to be real.<sup>3</sup> Despite these problems, the consensus is that SM-SERS is indeed possible. Although each piece of evidence in favor of SM-SERS is not a proof in itself, the accumulated body of evidence from different experiments gives, as a whole, a strong argument that it must be real. There remains the question however of how to determine, for a given SERS experiment, whether we are in a regime of single molecule SERS or not. This is a very important problem, since the interpretation of many recent SERS experiments rely on the fact that SM-SERS is observed, but do not provide an unambiguous proof that it is indeed the case.<sup>4,5</sup> One pre-requisite to observe SM-SERS is the existence of positions of large SERS enhancements, so-called hot-spots (HS's) on a SERS substrate. Suitable HS's are believed to be formed for example at a junction between two metallic nanoparticles,<sup>6,7,8</sup> and are highly localized.<sup>9</sup> This HS localization makes it very difficult to design experiments where SM-SERS signals are observed and unambiguously demonstrated.

The ideal approach would be to take one molecule and place it precisely at a HS, but there is currently no easy way of achieving this. Laser forces on the probe molecule could be an option but it has not yet been demonstrated experimentally to occur.<sup>10</sup> The probe molecule(s) therefore adsorb at a random position on the substrate. The most common approach currently relies on an ultra-low concentration of analyte, which ensures that one molecule (at most) will adsorb at the HS and in principle guarantees the single molecule nature of the detected signals. This approach presents several shortcomings. Firstly, it heavily relies on a correct estimate of the surface coverage of the analyte. This is often prone to errors, and can

be particularly deceitful for low concentration where wall adsorption during preparation or contamination can lead to large errors in the analyte concentration. Secondly, the probability that the single molecule adsorbs at a HS (the only place where it can be detected) is very small. This leads to very unreliable statistics (since most HS's are unoccupied) that would not pass even the simplest tests of statistical confidence. In practice, this approach may (at best) provide an indication of the presence of HS's with single molecule detection capabilities, but is not suited to carry out systematic SERS experiments using single molecules. In our opinion, the most convincing method based on ultra-low concentrations is possibly the one based on Langmuir-Blodgett monolayers, developed by Aroca and co-workers.<sup>11</sup> While suffering still from some of the drawbacks regarding the statistics of observed intensities, it is one of the methods that offers the largest degree of control over where the dyes are and how they are distributed over the sample.

Another possible approach is to use larger analyte concentrations to ensure that most HS's are occupied by one molecule at least (on average). This approach also has its drawbacks. Firstly, we need to address the question of how we know the concentration that is required to have one molecule at HS's on average. Secondly, even if we know the answer to the latter question, we now have many more molecules at non-HS positions on the substrate. A natural question then arises: How do we know if the SERS signal is dominated by these many molecules with a low EF, or by the one at the HS with a large EF? In many cases, the presence of fluctuations or of a Poisson distribution of intensities are taken as evidence for SM signals, and these questions are then ignored. In fact, these two questions are strongly intertwined with the EF distribution. By studying this distribution and its implication on the statistics of SERS signals, we will show that these arguments (Intensity fluctuations and Poisson distributions of intensity) are not always correct and need to be assessed carefully. An alternative method, which we recently developed, relies on the simultaneous use of two distinguishable analytes to answer these questions, at least experimentally.<sup>12</sup> This method is simple to im-

plement and provides a general recipe for proving the presence of SM-SERS signals under different experimental conditions. Moreover, this technique showed that the SERS signals from small colloidal clusters in liquids can be dominated by a few molecules only, even at fairly high concentration. This conclusion highlights the importance of the distribution of SERS enhancements in SM-SERS experiments and it is one of the aims of this paper to study this connection.

The distribution of enhancements in metallic structures is relevant to many other techniques exploiting local field enhancements, such as Surface Enhanced Fluorescence (SEF) and, to some extent, to plasmonics in general. Previous studies have concentrated mainly on the maximum local field enhancements that can be achieved, in particular at hot-spots. This approach is important, for example, to understand whether enhancements are sufficiently large to observe signals from single molecules. It is appropriate if one can easily place a molecule *exactly at the HS*. In most cases, however, molecules are randomly positioned, and it is therefore equally important to study what happens *around the HS* and with the overall distribution of enhancements.

We emphasize in this work the connection between the SM-SERS problem and the distribution of SERS enhancement factors (EF's) on a given substrate. Large SERS enhancements ( $\approx 10^8 - 10^{10}$ ) are required to detect a single molecule. There are currently no known SERS substrates that exhibit such large enhancements uniformly across the substrate. On the contrary, these large EFs are believed to occur precisely at HS's, typically located in a narrow gap between two metallic objects.<sup>6,7,8</sup> This can for example be at a junction between two metallic particles, or between a metallic tip and a metallic substrate in Tip-Enhanced Raman Scattering (TERS) experiments. Within this picture, the HS covers a small surface area compared to the rest of the substrate, but exhibits a much higher EF and should therefore contribute substantially to the signal. We will here quantify more carefully this assertion and put it in the context of several claims made in the past in the field of SM-SERS.

The paper is organized as follows: in Sec. II, we study the SERS enhancement distribution around a single hot-spot and discuss its main characteristics. The discussion is based on a representative example, and we propose a simple analytical model for the enhancement distribution. In Sec. III, we discuss how the EF distribution may change depending on the HS characteristics. In all cases, the main property of the EF distribution around a HS is its “long-tail” nature. In Sec. IV, we discuss the implications of these “long-tail” distributions for the statistics of SERS signals, in particular in the single molecule regime.

## II. ENHANCEMENT FACTOR DISTRIBUTION AT A GAP HOT-SPOT

### A. Presentation of the problem

In order to study how the enhancement distribution may affect the statistics of SERS signals, we first need to find the distribution itself in a situation where HS's are present and, in particular, in the case of one single HS. The strongest HS's, and therefore the ones required for SM detection, are believed to be “gap HS's”, formed at a junction between two closely spaced metallic objects.<sup>8</sup> We will therefore study a model system of two closely spaced spherical metallic particles.<sup>13,14</sup> This system presents a strong HS in between the two particles, as required, and captures essentially the physics of most “gap” HS's, formed by two closely spaced objects. The conclusions will therefore remain valid for more complex systems, qualitatively and semi-quantitatively.<sup>13,14</sup>

This electromagnetic problem can be solved analytically in 3D following Generalized Mie Theory as developed in Ref. 15, and the electromagnetic enhancements can therefore be calculated pseudo-analytically to a high accuracy. The series and matrices required for its solution were computed numerically, and we checked the convergence of the solution. The calculated EF's are therefore exact. This is important since many of the approximations used to solve such problems tend to have problems when estimating the local field enhancements, especially at HS's. This is because most numerical techniques, such as Finite Element Modelling<sup>16,17,18</sup> or the Discrete Dipole Approximation,<sup>19,20,21,22</sup> rely on a discretization (meshing) of the geometry. This gives satisfactory results in terms of far-field properties (scattering or extinction), but rapidly face limitations when computing the local field at the surface. This is because of the large field gradients existing at a HS, which require the use of an extremely fine mesh, often resulting in prohibitively large computational time for 3D simulations. 2D simulations can be useful in understanding qualitative effects<sup>23</sup>, but are unlikely to predict realistic enhancement factors for 3D structures.

The SERS electromagnetic enhancement factors,  $F(\mathbf{r})$  can be calculated at any position from the knowledge of the local field  $\mathbf{E}_{\text{Loc}}(\mathbf{r})$  (the incident field amplitude is denoted  $E_0$ ). It depends in principle on the Raman tensor of the probe, its adsorption geometry, the scattering geometry (e.g. backscattering), and the energy of the vibrational mode.<sup>24</sup> To avoid unnecessary complications, we use the approximation  $F \approx |\mathbf{E}_{\text{Loc}}/E_0|^4$ , which is simpler, more general, and sufficient for our purpose here. The meaning of this approximation has been discussed in Ref. 24. We will focus primarily on  $F$ , which represent the electromagnetic SERS enhancement factor, but it is easy to adapt our results to  $M = \sqrt{F}$ , i.e. local field intensity enhancement, which is important in other situations, such as enhanced absorption or SEF.

To illustrate our discussion, we will consider the spe-

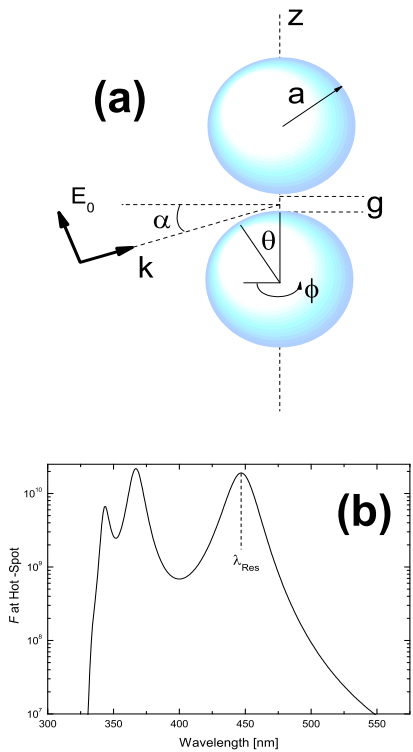


FIG. 1: (a) Schematic illustration of the electromagnetic problem under consideration: a dimer formed by two silver particles of radius  $a = 25$  nm and separated by a gap  $g = 2$  nm, excited by a plane wave polarized along the dimer axis ( $z$ ), i.e.  $\alpha = 0$ . Any position on the surface of the bottom particle are defined by standard spherical coordinates angles  $\theta$  (measured from the dimer axis) and  $\phi$  (measured from the incidence plane). (b) Calculated enhancement factor  $F = |E_{\text{Loc}}/E_0|^4$  at the surface of the bottom particle along the dimer axis (i.e. at the hot spot,  $\theta = 0$ ). The resonance at  $\lambda_{\text{Res}} = 448$  nm is a plasmon resonance resulting from the dipolar interaction between the two particles. The other peaks are due to higher order interaction. Note that  $F$  remain large over a wide range of wavelengths.

cific case of a dimer of two silver spheres in air excited in a configuration as shown schematically in Fig. 1(a). The polarization of the incident field is aligned along the dimer axis ( $\alpha = 0$ ). This is the configuration where the largest enhancement is predicted at the HS in the gap. The parameters used are as follows: radius  $a = 25$  nm, gap  $d = 2$  nm, and the local dielectric function of silver was used.<sup>25</sup> We show in Fig. 1(b) the wavelength dependence of the EF at the HS, i.e. at the surface of one of the particles along the dimer axis in the gap. The resonance due to dipolar interaction between the two spheres is the most red-shifted one, and occurs at  $\lambda \approx 448$  nm.

It would be further red-shifted to  $\approx 542$  nm in water and even further if the particles were not spheres. This resonance is the important one for SERS, and we therefore choose the excitation to be at  $\lambda = 448$  nm to study the EF distribution. The results are largely independent of this choice, as we shall see later.

Finally, we will only focus in this work on the distribution of EF's on the metallic surface. We therefore study the EF experienced by molecules directly adsorbed on the surface and ignore any effects of additional layers of molecule. It is generally believed that this first layer contributes to most of the SERS signal<sup>26</sup>. Moreover, in situations of single molecule detection, the concentration is well below monolayer coverage, hence justifying even further the choice. Note that we also neglect any chemical contribution to the SERS enhancement.

## B. Enhancement distribution at the surface

We calculated  $F$  for positions on the surface defined by  $0 \leq \theta \leq \pi$  (see Fig. 1(a)) and various  $\phi$  (note that the symmetry of revolution is broken here by the direction of the wave-vector of the incident beam, so there could be a  $\phi$  dependence). Because of the large variation of  $F$ , it is more convenient to characterize the EFs by  $L = \log_{10} F$ . We show the distribution  $L(\theta)$  in Fig. 2(a) for  $\phi = 0$  and  $\phi = \pi/2$ . It is clear that the results are virtually identical, especially in the region of interest (close to the HS). We will therefore ignore the  $\phi$  dependence in the following:  $L(\theta, \phi) \approx L(\theta, \phi = 0)$ . We also see in 2(a) a very sharp increase in the EF as one approaches the HS ( $\theta = 0$ ). The EF drops by a factor of 10 from  $\theta = 0$  to  $\theta = 0.19$  rad ( $11^\circ$ ). The maximum  $F$  in this example is  $F_{\text{max}} = 1.9 \times 10^{10}$  at the HS, while the minimum is  $1.5 \times 10^3$  for  $\theta = \pi/3$ . This clearly highlights the huge variation in  $F$  across the substrate, over 7 orders of magnitude here.

From the curve  $L(\theta)$ , we can in principle derive the EF distribution on the surface, i.e. the probability density function (pdf)  $p(F)$  that a molecule at a random position experiences a given enhancement  $F$  (strictly speaking  $p(F)dF$  is the probability that the enhancement is between  $F$  and  $F + dF$ ). To do so, we need to take into account the fact that the problem is in 3D with (approximate) symmetry of revolution. A given  $\theta$  corresponds to a ring on the sphere surface, whose radius varies with  $\theta$ . Therefore, if we pick a random position on the surface,  $\theta$  is not uniformly distributed, but has a pdf  $p(\theta) = (1/2) \sin \theta$ . The pdf  $p(F)$  for  $F$  can be expressed analytically as a function of  $F(\theta)$ . However, because we do not have here an analytical expression for  $F$ , but only its value for discrete  $\theta$ 's, it is easier to determine  $p(F)$  using a Monte-Carlo-type approach. We generate random  $\theta$  according to their probability distribution  $p(\theta)$  and for each of them calculate the corresponding  $F$  using a quadratic interpolation of the curve  $F(\theta)$  around  $\theta$ .  $p(F)$  and  $p(L)$  are then obtained by drawing a (normalized) histogram of the obtained  $F$  and  $L$ . Various repre-

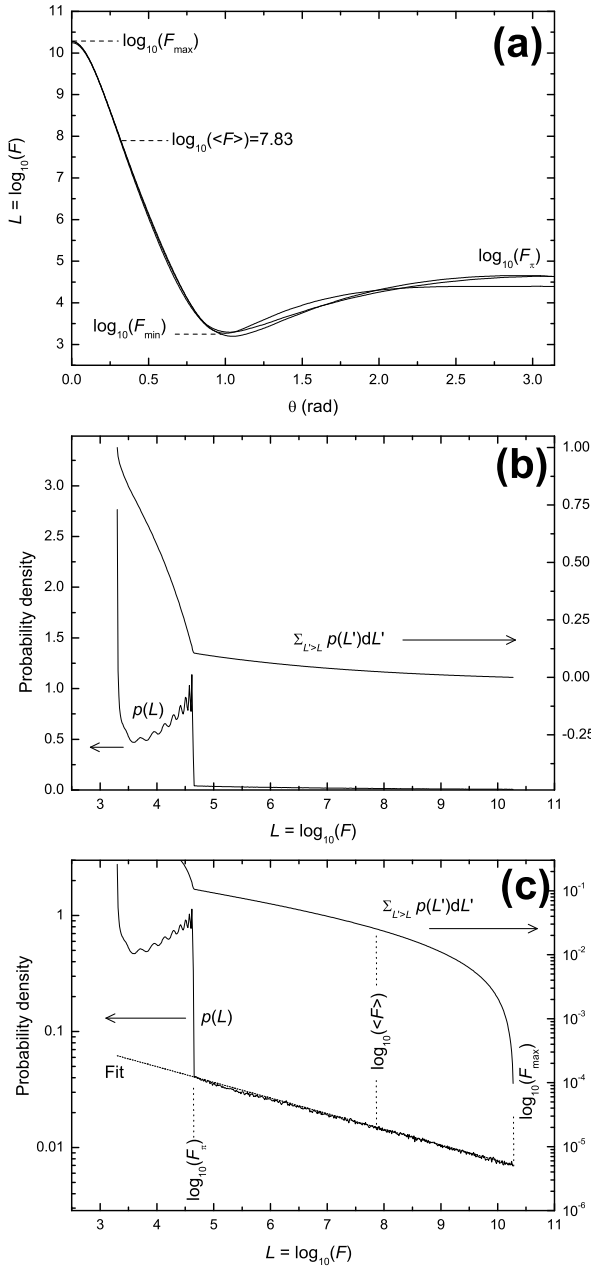


FIG. 2: Several representations of the EF distribution on the surface of one sphere of a dimer. Due to the many orders of magnitude spanned by  $F$ , the EF is characterized by  $L = \log_{10} F$ . (a)  $L$  as a function of  $\theta$  for  $\phi = 0$  and  $\phi = \pi/2$ . Also shown is the case  $\alpha = 45^\circ$  where the incident wave comes at a  $45^\circ$  angle with polarization at  $45^\circ$  from dimer axis (EF scaled here by a factor 4, see Sec. III A). The three curves are nearly identical, especially close to the HS ( $\theta = 0$ ). (b) Probability distribution function (pdf) of  $L$ ,  $p(L)$ , for a random distribution of molecules on the sphere.  $p(L)$  can be derived from  $L(\theta)$  taking into account the fact that  $p(\theta) = (1/2) \sin \theta$ . The quantity  $p(L' > L) = \sum_{L' > L} p(L')dL'$  (i.e. 1-cdf, where cdf is the cumulative distribution function) is also shown. The distribution is so skewed that the interesting region of large enhancement ( $L > 5$ ) can hardly be seen. (c) Same as (b) on a semi-log scale to highlight the tail of large enhancements. The fit to the pdf of a truncated Pareto distribution is also shown (dotted line).

sentations of this distribution are shown in Fig. 2(b-c). Note that we have to generate a large number of random  $\theta$  ( $10^7$  here) to produce smooth plots because the probability distribution is very skewed and spans a wide range. The average enhancement per molecule can be obtained in two equivalent ways, either using  $F(\theta)$  or  $p(F)$ :

$$\langle F \rangle = \int_0^\pi F(\theta) \frac{\sin \theta}{2} d\theta = \int F p(F) dF. \quad (1)$$

Both lead to  $\langle F \rangle = 6.7 \times 10^7$  in this case ( $\log_{10}\langle F \rangle = 7.83$ ). The average of the distribution is explicitly shown in Fig. 2(a) and it shows that it is completely dominated by the region close to the HS itself. The EF distribution shown in Fig. 2(a-c) captures all the important aspects of SERS enhancement around a single HS and their relation to statistical fluctuations, as we shall show in what follows.

### C. Principal characteristics of the EF distribution at a HS

We will now discuss several general important points. The main characteristic of the distribution  $p(F)$  is that it is a so-called “*long-tail* distribution”. It is similar in some ways to the Pareto distribution, encountered in many areas of physics, economy, and social sciences.<sup>27</sup> It is often used as a paradigm to model the wealth distribution in a society.<sup>28</sup> Fig. 2(a-c) actually reveal that SERS enhancements are some sort of an extreme example of a Pareto distribution (compared with the examples found in social sciences)<sup>28</sup>, because the enhancement is completely dominated by what happens in a very narrow angular range. We summarize the main characteristics of this distribution here:

- The average SERS enhancement is  $\langle F \rangle = 6.7 \times 10^7$ , which is about 285 times smaller than the maximum enhancement  $F_{\max} = 1.9 \times 10^{10}$ . This means that a single molecule exactly at the HS would contribute as much to the SERS signal as  $\sim 300$  randomly positioned molecules.
- For a uniform distribution of molecules on the surface, 80% of the SERS signal originates from only 0.64% of the molecules. These correspond to the molecules in a small disk-like region around the HS characterized by an angular spread of  $\theta < 0.16 \text{ rad } (9^\circ)$ . An equivalent version of the Pareto principle<sup>28</sup> for our system would be that: on average, 98% of the SERS signals originates from only 2% of the (randomly) adsorbed molecules.
- These considerations have immediate implications in terms of fluctuations of the signal. If one records the SERS signal in successive events, each originating from say 300 randomly adsorbed molecules, then strong fluctuations are automatically expected. This is because on average the signal will be

dominated by only 0.64% of these, i.e. 2 molecules. Fluctuations are therefore bound to arise depending on where exactly in the HS these two contributing molecules are adsorbed. We shall return to this issue later.

- The distribution has such inequalities that the contribution from molecules far from the HS is always negligible. Despite the fact that there could be a large number of them (say 1000 times more than close to the HS), their enhancement factor is so small (at least  $10^5$  smaller) that their contribution can be safely ignored. In other words, the exact form of the distribution  $p(L)$  for say  $L < 6$  has no impact on most observations.

#### D. A simple model hot-spot

This last remark is in fact quite useful, because it enables us to model the distribution with analytical expressions with only 3 parameters. First, we see in Fig. 2(c) that the tail for large  $L$  can be well-approximated by a straight line. This means that:

$$\log_{10} p(L) \approx -kL + c. \quad (2)$$

Using the fact that  $p(F) = p(L)/(F \ln(10))$ , this leads to the empirical formula:

$$p(F) \approx AF^{-(1+k)}. \quad (3)$$

In our example, we extract  $k \approx 0.135$  and  $A \approx 0.075$ . The corresponding fit is shown in Fig. 2(c). This expression is similar to that of the pdf for a Pareto distribution. There is a difference, however, in the value of  $A$  because our distribution does not extend to  $F \rightarrow \infty$ , but has a maximum value:  $p(F) = 0$  for  $F > F_{\max}$ , corresponding to the maximum physically achievable enhancement in the sample. Therefore, it corresponds to a *truncated Pareto distribution* (TPD). Under these conditions, we can approximate the enhancement distribution by a TPD with 3 parameters:  $k$ ,  $A$ , and  $F_{\max}$ . This distribution is very accurate for large enhancements  $L > 5$ , but not for lower enhancements (see Fig. 2(c)). We have already emphasized, nevertheless, the fact that lower enhancements have a negligible contribution, so this approximate distribution is in fact excellent for most predictions, regardless of how the distribution is extended to lower enhancements.

The approach we describe is, in fact, a very general approach for characterizing SERS enhancements in a substrate containing HS's. All important physical predictions can be deduced from the value of these three parameters. The mathematical details of such derivation are presented in Appendix A. In our example, we have  $k = 0.135$ ,  $A = 0.075$ , and  $F_{\max} = 1.9 \times 10^{10}$ . With these parameters, we can (for example) re-derive from Eq. (A6) the previously obtained average of  $\langle F \rangle = 6.7 \times 10^7$ .

We now discuss briefly the physical meaning of these three parameters for a given HS:

- $F_{\max}$  simply describes the maximum intensity of the HS and can be viewed as the “strength” of the hot spot. It is the enhancement experienced by a molecule placed exactly at the right spot. This needs to be sufficiently large if SM-signals are to be detected.
- $A$  is an indication of how probable it is for a molecule to be located at (or close to) the HS. In a way,  $A$  is not really a characteristic of the HS itself but more of the remaining metallic surface. It is a representation of the relative area of the HS with respect to the rest of the substrate. In simple terms, the larger the value of  $A$ , the larger the hot-spot area with respect to the rest. The current description (with a truncated Pareto distribution) would fail though if  $A$  is too large, since the HS would then not have enough “contrast” in enhancement with respect to the rest in order to be considered as a proper hot-spot.
- $k$  determines how fast the enhancement decreases when moving away from the HS. It is therefore (indirectly) a measure of the sharpness of the resonance (in spatial terms) of the HS. To visualize this, let us consider for example the number of molecules experiencing an enhancement  $F = F_{\max}/10$ . These molecules are all located at the same angle  $\theta$  from the HS (which is  $\theta = 0$  in Fig. 1(a)), i.e. they form a ring around the HS. The number of these molecules increases with  $\theta$ . It should also be proportional to  $p(F_{\max}/10) = A(10/F_{\max})^{1+k}$ , which is decreasing with  $k$ . When  $k$  increases, the corresponding ring must then be smaller (i.e. smaller  $\theta$ 's), and the spatial resonance is sharper. A larger  $k$ , for the same  $A$  and  $F_{\max}$ , therefore corresponds to a sharper resonance, with larger enhancement gradients. Note however, that for general values of  $k$ ,  $A$  and  $F_{\max}$ , the sharpness of the resonance is better characterized by the value of  $D$  given in Eq. (A7) (large  $D$  for sharper resonances).

#### E. Enhancement Localization

It is often stated in the SERS literature that HS's are places of highly localized enhancements on the surface. We can now quantify this assertion using our model HS. We define the  $q$ -HS ( $0 \leq q \leq 1$ ) as the region around the HS from which a proportion  $q$  of the total SERS signal originates, and denote  $a_q$  its area relative to the total surface area. For example,  $a_{80\%}$  is the relative area on the substrate from which, on average, 80% of the signal originates. If the HS is strong and highly localized, then  $a_q$  should be small, even for  $q$  close to 1 (most of the signal originates from a very small region). Note that by

TABLE I: Characteristics of  $q$ -HS's for the example considered here. The  $q$ -HS's are disk-like regions around the HS from which a proportion  $q$  of the total SERS signal originates. They are defined as  $\theta < \theta_q$  (see Fig. 1(a) for the definition of  $\theta$ ).  $F_q$  is the enhancement at the edge ( $\theta = \theta_q$ ) and  $a_q$  is the relative area of the  $q$ -HS. See Appendix A for derivation of these values.

$q$	$F_{\max}/F_q$	$a_q$	$\theta_q$ (°)
50%	2.23	0.26%	5.8
80%	6.43	0.64%	9.2
90%	14.3	0.97%	11.3
95%	32.0	1.34%	13.3
98%	92.3	1.89%	15.8
99%	206.0	2.37%	17.7

definition,  $a_{100\%} = 100\%$ . General expressions for  $a_q$  are given in Appendix A as a function of the HS parameters. Examples of the relative areas of  $q$ -HS for our example are given in Table I. These numbers confirm the figure quoted in the previous discussion.

### III. HOT-SPOT TO HOT-SPOT VARIATION

We have so far focused on describing one single HS. This approach is relevant to many experimental situations. In particular, for SM-SERS studies, the experimental conditions are usually adjusted to achieve exactly this, a maximum of one HS at a time in the scattering volume. There are however other situations where the signals will originate from a substrate containing many hot-spots, for example in a large colloidal aggregate. In such conditions, the single HS model is still useful since the total signal can in a first approximation be taken as the sum of signals from independent hot spots. It is however necessary to understand how the enhancement distributions may change from one HS to another. This study is also necessary to understand series of measurements where one single HS may be measured at any given time, but not necessarily the same one each time.

#### A. Incident polarization effects

The first obvious source of variation from one HS to another is the variation in the orientation of the incident field polarization. It is well known that gap HS's are highly uniaxial,<sup>14</sup> and optimal enhancements are obtained when the incident field polarization matches the HS axis. In the previous study of our model HS, we assumed that the incident field was along the dimer axis, i.e. optimum coupling. In a more general case, the results depend on both the incident wave-vector direction and polarization. In a first approximation, the dimer has a response similar to a dipole<sup>13,14</sup>, and only the angle  $\alpha$  between polarization and dimer axis is important, introducing an additional factor  $\cos^4 \alpha$  to the enhancement.

Such an example is shown in Fig. 2(a) for  $\alpha = 45^\circ$ . The corresponding curve  $F(\theta)$  is nearly identical to that obtained for  $\alpha = 0$ , only scaled by a factor  $\cos^4 \alpha = 1/4$ .

Denoting  $F_0(\theta)$  the EF for  $\alpha = 0$ , we then have  $F(\theta, \alpha) = F_0(\theta) \cos^4 \alpha$ . We assume  $F_0$  follows the probability distribution described previously, a TPD with parameters  $k$ ,  $F_{\max}$ , and  $A$ . In an experiment where one single HS with a fixed  $\alpha$  is observed, then  $F$  follows like  $F_0$  a TPD with the same  $k$ , but with  $F_{\max}$  reduced to  $F_{\max} \cos^4 \alpha$ , and  $A$  to  $A \cos^4 \alpha$ . In many situations, the angle  $\alpha$  is however not fixed. For a random orientation of the dimer axis,  $\alpha$  is also a random variable with probability  $p(\alpha) = (1/2) \sin \alpha$ . We can then derive the probability distribution of  $F$  and we find that  $F$  again follows a TPD, with the same parameters  $k$  and  $F_{\max}$ , but where  $A$  is replaced by  $A/(1 + 4k)$ .

Overall, the previous arguments show that the incident polarization effects do not significantly change the conclusions drawn earlier. The EF distribution still follows a TPD with the same  $k$  parameter. Only small changes to the other two parameters apply, transforming them into “effective” parameters averaged over the incident polarization directions.

#### B. Different types of HS

We now briefly study how the distribution may vary for different types of gap HS's. Within our model gap HS formed by a dimer, one could expect the distribution to change with a number of parameters: wavelength  $\lambda$ , separation (gap) between particles  $g$ , radius of particles  $a$ , optical properties of the metal. We carried out calculations of the EF distributions for various combinations of these parameters. The first observation is that for all cases studied here, the distribution of EF is always “long-tail” and extremely well-represented by a TPD (in the high EF region), as in the example studied previously. Like in many other cases in SERS, one could argue that the example of a dimer captures the essence of most high enhancement situations, irrespective of the details. The parameters of the TPD for a number of representative cases are summarized in Table II.

The most interesting aspects of this table are briefly discussed:

- The main difference among HS's appears in the value of  $F_{\max}$ , which varies by 3-4 orders of magnitude here. However, this variation only reflects a global scaling factor on the whole distribution of enhancement, not on its shape. For example, the average enhancement scales by approximately the same amount.
- $F_{\max}$  describes the strength of the HS and it is stronger in the following situations: (i) for silver compared to gold, (ii) when the excitation wavelength matches the (red-shifted) plasmon resonance of the dimer, (iii) for smaller gaps, and (iv) for

TABLE II: Example of various gap HS's formed by two closely-spaced metallic particles excited with a field polarized along the dimer axis. The HS's characteristics depend on a number of parameters: metal (silver or gold), radius  $a$  of each particle, gap  $g$  between particles, and excitation wavelength  $\lambda$ . The (R) after  $\lambda$  indicates that this particular wavelength corresponds to the plasmon resonance of the dimer (where the maximum enhancements are obtained). The enhancement distribution can be fitted to a truncated Pareto distribution with parameters  $k$ ,  $F_{\max}$ , and  $A$ . The sharpness and localization can be further described by the values of  $D$  and  $a_q$  (defined in the text and in Appendix A).

Metal	HS characteristics			TPD parameters				
	$a$ (nm)	$g$ (nm)	$\lambda$ (nm)	$k$	$F_{\max}$	$A$	$D$	$a_{80\%}$
Ag	25	2	447 (R)	0.135	$1.9 \times 10^{10}$	0.075	285	0.64%
Ag	25	2	467	0.152	$2.3 \times 10^9$	0.086	258	0.72%
Ag	25	3	429 (R)	0.148	$2.5 \times 10^9$	0.114	183	1.01%
Ag	25	3	447	0.156	$4.3 \times 10^8$	0.113	166	1.13%
Ag	25	1	486 (R)	0.128	$6.5 \times 10^{11}$	0.055	512	0.35%
Ag	12.5	1	429 (R)	0.120	$4.2 \times 10^{11}$	0.066	327	0.55%
Au	25	2	558 (R)	0.163	$1.0 \times 10^8$	0.068	248	0.76%

larger curvature around the HS (i.e when  $a$  is smaller). These four aspects manifest themselves here in the specific context we are studying, but are in fact well-known in the general picture of field enhancements in metallic nano-structures.

- The most remarkable feature, however, is in the actual distribution of enhancements. The parameters  $k$  and  $A$  do not vary much from one HS to another, even for relatively large variation of the gap  $g$ , or changing from silver to gold (which leads to a change from 0.26 to 2.0 in the imaginary part of the dielectric function  $\epsilon(\lambda)$  at the wavelengths considered here).

To summarize this section, the shape of the enhancement distribution remains in a first approximation independent of the HS characteristics. The HS strength is therefore the dominant parameter in the variability from one HS to another. Hence, the considerations of the previous sections apply to a wide variety of gap HS's. The distribution is always extremely skewed ("long-tail") with a  $k$  parameter in the range  $\sim 0.12 - 0.18$ , and is simply displaced towards the lower or higher enhancements region depending on the actual strength of the HS. This conclusion, we believe, will hold for most types of gap HS's.

Note finally that one could consider other types of HS's, such as those formed in a groove, or at sharp corners. These HS's are not as strong and therefore less likely to be relevant to SM-SERS studies. The "long-tail" nature of the distribution will remain, but the parameters could change compared to gap HS's. These would require a separate study.

### C. Collection of hot-spots

As mentioned before, there are experimental situations where a large number of HS's are present. We will not

dwell on this aspect here since it is less relevant to SM-SERS, but simply make a few general remarks.

In most situations involving a large number of HS's, the substrate may be considered as a collection of spatially separated independent single HS's. The distribution of EF's can then in a first approximation be obtained by summing the contribution from these HS's (i.e. summing their respective pdf's). Note however that the HS's can come from regions which will have in general different relative areas, and the sum should therefore be weighed to take this into account. Such a weight factor can modify the  $A$  parameters of the various  $p(F)$ . The other main difference between the various  $p(F)$  can come from different  $F_{\max}$ , which may vary, say by  $\sim 3 - 4$  orders of magnitude depending on the HS strength, and incident polarization. In order to be quantitative in such a situation, one would need to assume a distribution of  $F_{\max}$ 's and then estimate the sum of the various  $p(F)$ 's. If the  $F_{\max}$ 's are relatively uniform across HS's, the total EF distribution will simply resemble that of a single HS with a  $k$  parameter in the range  $\sim 0.12 - 0.18$ , as before. If the  $F_{\max}$ 's vary over several orders of magnitude, then a decreasing number of HS's contribute to the distribution at higher enhancements. This will result in a slight "bending" of the straight line representing  $\log_{10} p(L)$  in Fig. 2(c) in the region of large  $L$ 's. The distribution remains highly skewed and similar to a Pareto distribution, but this could increase the value of the  $k$  parameter in the region of interest (high enhancements).

## IV. STATISTICS OF SERS SIGNALS

We now focus on the consequences of the distribution of SERS enhancements on the signal statistics. We have seen that this distribution is always highly skewed when HSs are present, and can be modelled as a truncated Pareto distribution in most cases of interest. We will therefore again use the same example of HS's as in the previous section to illustrate our arguments, but the fol-

lowing considerations are fairly general and apply to any system containing HS's (and therefore a "long-tail" distribution of enhancements). It is particularly appropriate to single molecule SERS experiments, where single HS's are usually studied. As before, we consider in the following a model HS, here with  $N_{\text{mol}}$  molecules randomly positioned on the surface. We assume that a series of SERS measurements is carried out on this system and analyze the statistics of the SERS signals; a situation that has been studied experimentally in the context of SM-SERS in countless opportunities. To the very best of our knowledge, there has never been a serious attempt to pin down the physical meaning of the statistics of events in these experiments by means of a model distribution for the enhancements at HS's. The next subsections, therefore, present some of the key results of the analysis using the tools developed so far.

### A. Ultra-low concentration

Let us first consider the extreme case of  $N_{\text{mol}} = 1$ . Note that in most SM-SERS experiments, it is claimed that there is indeed less than one molecule at a time in the scattering volume.<sup>1,2</sup> In this case, the SERS signal from this molecule will only be detected if it is located at a position of sufficiently high enhancement  $F > F_t$ , i.e. close to the HS, where  $F_t$  depends on the sensitivity of the detection and the intrinsic scattering properties of the probe. Let us assume, for example, that only molecules experiencing an EF of  $F_t \approx F_{\max}/100$  or more can be detected (note that this is a very optimistic estimate). Then one can see that  $p(F > F_t) = a_{99\%} \approx 2.37\%$ , i.e. a signal will be observed for only 1 event in every 42. Moreover, the intensity of these events will fluctuate by a factor of around 100, depending on exactly where the observed molecule is located in the HS. Using a more realistic factor (10 instead of 100), only one SM event in every 100 is detectable. Such a behavior was observed experimentally by Nie *et al.*<sup>1</sup>. Only a small proportion of the colloids were active, i.e. only the ones where the molecule was by chance at the HS. In the limit of ultra-low concentrations, it is then extremely difficult to demonstrate that the number of detected events scales with concentration due to the worsening statistical significance. This opens the door to alternative explanations based on "rare events" which are not necessarily SM.

### B. Medium concentrations

It is now interesting to study what happens for more than one molecule on the surface and see whether the fluctuations can be averaged out by having several molecules instead of one. A simple approach is to consider  $a_{50\%}$ , which is the relative area from which 50% of the SERS signal originates. If we have on average only one molecule in this small area (corresponding to

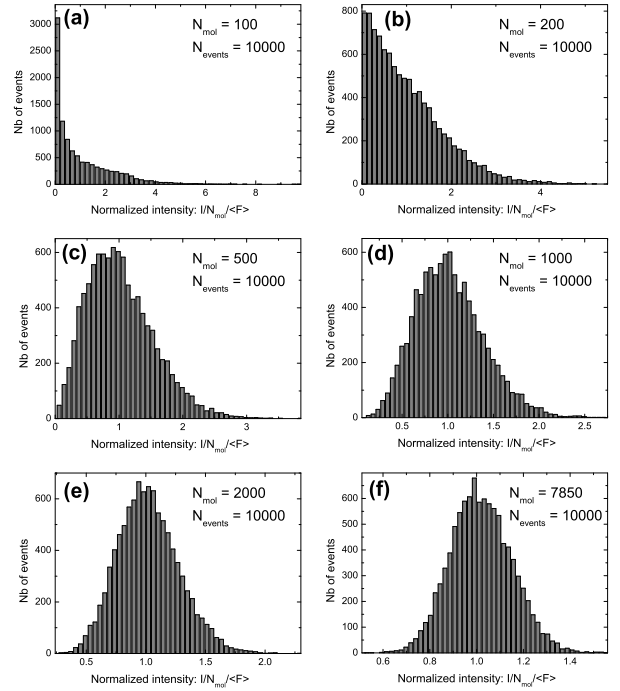


FIG. 3: Statistics of SERS signals for events consisting of  $N_{\text{mol}}$  randomly adsorbed molecules on a SERS substrate consisting of the model hot-spot described in Sec. II. Each histogram is calculated from 10000 events. They represent the distribution of normalized SERS intensity  $I_N = (\sum_{i=1}^{N_{\text{mol}}} F_i)/(N_{\text{mol}} \langle F \rangle)$ . The average value for all is therefore  $\langle I \rangle = 1$ . The scale for each histogram is adjusted from  $I_{\min}$  to  $I_{\max}$  (the bars may not be visible if there are only a few events). Long-tail distributions are obtained up to  $N_{\text{mol}} = 500$  and remain asymmetric up to  $N_{\text{mol}} = 2000$ .

$N_{\text{mol}} \approx 1/a_{50\%}$ ), then we should typically expect fluctuations of the order of a factor of  $\sim 2$  (depending whether zero, one, or two molecules are in this area). In our example,  $a_{50\%} \approx 0.26\%$ , so  $N_{\text{mol}} \approx 250$ . We therefore expect substantial fluctuations even for 250 molecules on the surface. This is simply due to the nature of the enhancement distribution.

To understand further the statistics of SERS signals, we would ideally like to determine the probability distribution of the total intensity of  $N_{\text{mol}}$  randomly distributed molecules. This is a standard problem in probability theory: finding the pdf of the sum of  $N$  random variables with a known pdf. Unfortunately, there is no simple analytical expression (to our knowledge) for a sum of random variables with a truncated Pareto distribution. The easiest approach then is to compute numerically a histogram of SERS intensities for a large number of events of  $N_{\text{mol}}$  randomly distributed molecules. This represents the expected intensity distribution in an experiment with an average of  $N_{\text{mol}}$  molecules on the surface. Examples of such intensity distributions are shown in Fig. 3 for our model HS and various values of  $N_{\text{mol}}$ . The  $x$  axis in these histograms shows the intensity normalized with respect

to the number of molecules and to the expected average signal per molecule  $\langle F \rangle$ . A value of 1 therefore corresponds to the average signal. The smallest and largest value on the  $x$  axis corresponds to the intensities of the smallest and largest event (if there is only one such event, the bar in the histogram is too small to be visible).

We can make a number of remarks on these distributions:

- The distribution remains skewed (“long-tail”) even for large numbers of adsorbed molecules (at least 500 molecules). Large intensity fluctuations should therefore be expected in this range. As discussed before, this is due to the strong localization of the HS. The observed SERS intensity for 500 molecules has in fact a strong contribution from the few molecules (possibly one or two) closest to the HS. It is therefore not surprising to have fluctuations depending on the exact number and position of these few molecules. This is probably one of the most widespread experimental situations in SERS: low (but not ultra-low) concentrations.
- Even for 1000 or 2000 molecules, there is still an asymmetry in the distribution, i.e a long tail with a small probability of large events. This should be viewed as an intrinsic property of any HS-containing SERS substrate. The Pareto-like distribution of enhancements will always lead to a distribution of SERS intensities with a high-intensity tail, similar to a *lognormal* or *Gamma* distribution. This is true even for relatively large numbers of molecules and would only disappear for extremely large values (for example  $N_{\text{mol}} = 7850$  in the figure) where the central-limit theorem prediction of a Gaussian distribution is recovered.
- For small numbers of molecules, for example,  $N_{\text{mol}} = 100$ , there are many events with intensities below the detection limit. They correspond to events where no molecule is close enough to the HS to experience a sufficient enhancement. At such concentrations, the SERS signals originate essentially from a single molecule (the other 99 have a much smaller contribution). SM-SERS is therefore possible (and in fact much more practical) at concentrations much larger than typically used in ultra-low concentration studies. Decreasing further the concentration, as often done in SM-SERS experiments, will only decrease the probability of SM-SERS events and make the analysis more difficult and the statistics unreliable. The only issue at intermediate concentrations is to be able to prove that the signals are indeed SM signals. A bi-analyte technique as described in Ref. 12, or an equivalent method, must then be used to verify the SM nature of the signals.

It is clear from these examples that intensity fluctuations are an intrinsic property of SERS in most sub-

strates with HS’s. It is important to realize that they are not only a consequence of the variability of the SERS substrates itself. Even in a solution of exactly identical metallic dimers for example, fluctuations will arise for  $N_{\text{mol}} < 1000$  molecules per colloids simply as a result of the random adsorption combined with the highly skewed (“long-tail”) distribution of SERS enhancements. *Intensity fluctuations alone cannot be invoked as a proof of SM-SERS.*

### C. High concentrations

It is interesting to see whether it is possible to minimize or eliminate these fluctuations. If one could have a large amount of molecules on the surface, then the observed SERS signal should be  $N_{\text{mol}}\langle F \rangle$  with little fluctuations. An interesting question is how many molecules we need to remove the fluctuations. We could try to use the central limit theorem to answer this question but the distribution is so skewed that it may not apply except for very large  $N$  (slow convergence); a property that is clearly hinted at in Fig. 3. If it did apply, it would tell us that for sufficiently large  $N$ , the fluctuations around  $N\langle F \rangle$  are of the order of  $\sigma\sqrt{N}$ . If we define the term “small fluctuations” by the condition  $\sigma/(\sqrt{N}\langle F \rangle) \leq 10\%$ , this then requires to take  $N \geq 100(\sigma/\langle F \rangle)^2$ . An important aspect of long-tail distributions is that the standard deviation,  $\sigma$ , is very large, even much larger than  $\langle F \rangle$  in many cases (see Appendix A). In our example, we therefore need  $N > 13000$  !! This very large number again demonstrates the highly unusual nature of distribution we are dealing with for HS’s.

Now it is worth remembering that in SERS, we cannot in general have as many molecules as we want on a substrate’s surface. If we assume that only the first layer is active<sup>26</sup>, then the maximum number of molecules depends on the surface area of one molecule compared to that of the whole substrate. If we consider molecules with surface coverage of  $\sim 1 \text{ nm}^2$  (reasonable for dyes), and our model HS, which has a total surface of  $S = 7850 \text{ nm}^2$ , then  $N_{\text{max}}$  is of the order of 8000. The fluctuations are then reasonably small but still present (see Fig. 3(f)). Moreover, for many dyes in colloidal solutions, the maximum concentration can be limited by induced aggregation of colloids and fluctuations may then be unavoidable, even for the largest allowed concentrations. The SERS fluctuations can then be viewed as an unavoidable (and natural) consequence of the long-tail distribution of enhancements around HS’s.

### D. How to interpret “Poisson distributions of SERS intensities”?

A Poisson distribution of SERS intensities is often put forward as an argument for SERS SM-signals.<sup>2,29,30</sup> It was indeed one of the main arguments of one of the first re-

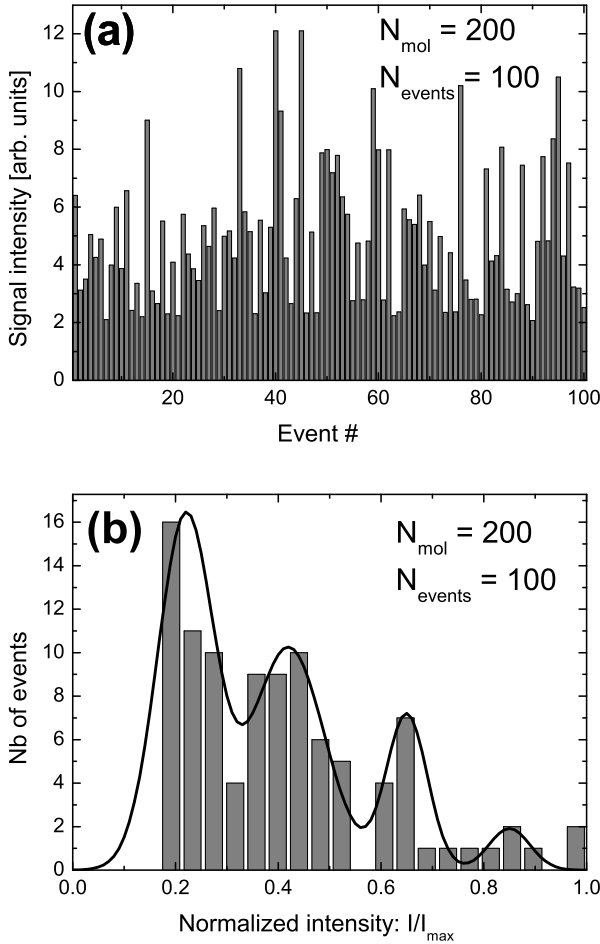


FIG. 4: Illustration of how a Poisson-like distribution is obtained from a random sample of 100 events for 200 randomly adsorbed molecules. (a) Fluctuations of the SERS intensity, where a background intensity of 2 has been added to resemble a typical SM-SERS experiment. (b) Histogram of intensities of the 100 events, together with a “Poisson” fit with Gaussian broadening. The “Poisson” parameter in this fit is 0.8. The Poisson-like nature of this histogram is artificial and due to the poor sampling (100 events). Taking 10000 events results in the histogram of Fig. 3(b).

ports on SM-SERS.<sup>2</sup> It is in general argued that the peaks in the Poisson distribution are a result of seeing none (background signal), one, two, or three molecules during a given SERS event. The average number of molecules can then be inferred from the relative intensities of these Poisson peaks. The conditions for this argument to be true have not been emphasized enough in our opinion:

- The argument is only valid if each single molecule gives exactly the same SERS signal (within less than a factor of 2 to differentiate between one strong molecule and two weak molecules). This is highly unlikely in SERS for many reasons: non-uniform exciting beam, changing orientation of substrate and/or molecule with respect to incident polarization, and most importantly the large spread

in the distribution of SERS enhancements.

- One could argue that there is a saturation mechanism, for example photo-bleaching of the molecule, which guarantees that every single molecule emits more or less the same signal before being destroyed. However, the photo-bleaching mechanisms under SERS conditions are still not well understood and it is not clear whether it would result in such a perfect saturation of the SERS signal from a single molecule (which follows a different enhancement factor than absorption or fluorescence).
- Even in the presence of a suitable saturation mechanism, the concentration inferred from the Poisson distribution would be much smaller than the experimental molecular concentration. This is because of the strong spatial localization of the HS: the chances of a molecule being at a HS are small, and the molecule is undetectable if it is outside the HS.
- If the concentration inferred from the Poisson distribution matches the experimental concentration, as in Ref. 2, then it means that every single molecule is adsorbed at the HS. This is very unlikely in general. It has been suggested that laser forces attracting the molecule towards the HS’s<sup>10,31</sup> could provide an additional mechanism to improve the chances of seeing molecules at HS’s, but this remains very speculative at the moment. In most studied situations it will be the surface chemistry and molecular interaction of the molecule with the surface that determines the way the analyte is spread over the surface.

We here propose a simpler, and arguably more credible, interpretation of these Poisson distributions. Let us first note that they are always obtained *from a small number of events*, 100 in general.<sup>2,29,30</sup> It is in fact a property of long-tail distributions that most random samples of  $\sim 100$  events exhibit peaks similar to a Poisson distribution. *This is true for any long-tail distributions*, such as lognormal distributions or those shown for example in Fig. 3(a-c) for  $N_{\text{mol}} \leq 500$ . To illustrate this, we show in Fig. 4 an example of the SERS intensities of 100 events for 200 molecules randomly distributed on the surface, along with a “Poisson” fit to the data. This fit is misleading, because it is only a result of the poor sample size used for the histograms (100 events). In fact, when using 10000 events, we simply obtain the histogram of Fig. 3(b), which is a “standard” long-tail distribution. This type of “Poisson” fits is therefore not a proof of SM-SERS, but rather illustrates the wide range of enhancements in a typical SERS experiments with HS’s and is another manifestation of the peculiar nature of the distribution present in this problem.

### E. Other experimental consequences of the EF distribution

We briefly discuss here two additional effects related to the enhancement distribution: vibrational pumping<sup>32,33,34,35,36,37,38</sup> and photo-bleaching under SERS conditions.

We have recently proposed a clear demonstration of the existence of vibrational pumping under SERS conditions.<sup>37,38</sup> This effect can in principle be used to extract the SERS cross-section of the analyte, and therefore the SERS enhancement. For a non-uniform distribution of enhancements, we have shown<sup>37,38</sup> that what is measured is not the average enhancement  $\langle F \rangle$ , but the pumping enhancement given by  $F_p = \langle F^2 \rangle / \langle F \rangle$  and argued that it was a good (under)estimate of the maximum enhancement  $F_{\max}$ . Using the truncated Pareto distribution of enhancement, we can give a more accurate estimate. Using Eq. (A8) and the fact that  $k$  is small, we deduce that the pumping enhancement,  $F_p$ , is approximately a factor of  $\sim 2$  smaller than the maximum enhancement.

Another phenomenon where the distribution of enhancement is likely to play an important role is photo-bleaching under SERS conditions. For conventional photo-bleaching, the number of molecules (and therefore the intensity) decays as  $n(t) = n_0 \exp(-\Gamma t)$  where the decay rate  $\Gamma$  depends on the laser intensity, in a first approximation as  $\Gamma = \beta I_L$ . The mechanisms of photo-bleaching under SERS conditions are still not well resolved, but it is reasonable to assume that  $\Gamma$  will also depend on the enhancement factor  $F$  experienced by the molecule. Two simple assumptions are  $\Gamma(F) = \beta F I_L$  (proportional to SERS EF), or  $\Gamma(F) = \beta \sqrt{F} I_L$  (proportional to absorption or local field intensity enhancement). This dependence would result in both cases in a non-exponential decay of the SERS intensity, which can be estimated from:

$$I(t) = N_{\text{mol}} \int p(F) F e^{-\Gamma(F)t} dF. \quad (4)$$

This equation in fact provides a starting point for using photo-bleaching as a way of measuring EF distributions experimentally. Combined with theoretical estimations of EF distributions, it also provides a chance of studying the photo-bleaching mechanism itself, i.e. determining the dependence  $\Gamma(F)$  and its physical origin. As an example, for a TPD as considered here, the expected decay of  $I(t)$  (for long times) are approximately power laws scaling as  $1/t^{1-k}$  if  $\Gamma(F) = \beta F I_L$  or as  $1/t^{2-2k}$  if  $\Gamma(F) = \beta \sqrt{F} I_L$ .

### V. CONCLUSION

The main purpose of this paper was to study the distribution of enhancements for HS's in SERS and to understand some very general properties. We have shown

that most problems on the statistics of signals coming from HS's and SM-SERS in general can be tracked down to the existence of a *very skewed* (long-tail) distribution of enhancements. Within this framework a series of natural consequences and explanations arise, among them: (i) the role and meaning of fluctuations at ultra-low concentrations, (ii) a proper justification of SM signals at medium concentrations (which is a justification for the bi-analyte method for SM-SERS developed in Ref. 12 at the same time), and (iii) the observation of probability distribution oscillations ("Poisson"-like), which are not by themselves a proof of SM-SERS but have their origin in the very peculiar characteristics of long-tail distributions. We also explored very briefly some of the consequences that the distribution of enhancement would have in vibrational pumping and photobleaching under SERS conditions. This latter predictions will have to await for experimental confirmation before further development is justified.

Overall, the approach taken here has the advantage of its "universal" nature in view of the fact that a power law distribution of enhancements is most likely to exist in SM-SERS substrates with HS's, independent of the exact details of the situation. This provides, therefore, not only a general understanding and a theoretical framework (in a field that has been plagued with diverging interpretations), but also a powerful phenomenological tool to describe the statistics of SM-SERS signals with a minimum set of parameters.

### APPENDIX A

We here consider the model distribution of enhancement for a single HS as defined by a truncated Pareto distribution with parameters  $k$ ,  $A$ , and  $F_{\max}$ . The parameters obtained in the example of Sec. II will be used for illustration:  $k = 0.135$ ,  $A = 0.075$ , and  $F_{\max} = 1.9 \times 10^{10}$ .

The pdf of the SERS enhancement factors,  $F$ , is then given by:

$$p(F) = AF^{-(1+k)} \quad \text{for } F_{\min} < F < F_{\max}. \quad (A1)$$

We have introduced here a minimum value for  $F$ ,  $F_{\min}$ , which is required for  $p(F)$  to be a valid pdf.  $F_{\min}$  can be deduced from the parameters using the normalization condition for the pdf,

$$\int_{F_{\min}}^{F_{\max}} p(F) dF = 1, \quad (A2)$$

which implies that

$$F_{\min} = \exp\left(-\frac{1}{k} \ln\left(\frac{k}{A}\right)\right). \quad (A3)$$

Note that  $F_{\min}$  is only introduced for mathematical consistency in the definition of  $p(F)$ , it has no physical meaning and will be irrelevant in all predictions. Its value is

typically very small (and in fact much smaller than the real physical minimum enhancement on the surface). For our example,  $F_{\min} \approx 7.6 \times 10^{-3}$ .

Equivalent representations of the EF distribution can be given in terms of  $L = \log_{10} F$ , for which

$$p(L) = A \ln(10) 10^{-kL}, \quad (\text{A4})$$

or in terms of the local field intensity enhancement  $M = \sqrt{F}$ , for which

$$p(M) = 2AM^{-(1+2k)}. \quad (\text{A5})$$

Other quantities of interest that can be derived are, firstly the average enhancement,  $\langle F \rangle$ , given by

$$\langle F \rangle = \int_{F_{\min}}^{F_{\max}} F p(F) dF \approx \frac{AF_{\max}^{1-k}}{1-k}. \quad (\text{A6})$$

It can also be written as:

$$\langle F \rangle = \frac{F_{\max}}{D} \quad \text{with} \quad D = \frac{1-k}{A} F_{\max}^k \quad (\text{A7})$$

$D$  characterizes the strength of the HS with respect to the average enhancements, and is usually quite large ( $D = 285$  in our example). This is a defining characteristics of all long-tail probability distributions.

One can also show that:

$$\langle F^2 \rangle = c F_{\max} \langle F \rangle \quad \text{with} \quad c = \frac{1-k}{2-k} \quad (\text{A8})$$

Note that  $c \approx 1/2$  when  $k$  is small, which is often the case ( $c \approx 1/2.16$  in our example). Moreover, using Eq. (A7) and the fact that  $D \gg 1$ , we derive the standard deviation  $\sigma$  of  $F$ :

$$\sigma \approx \sqrt{cD} \langle F \rangle. \quad (\text{A9})$$

$\sigma$  is therefore much larger than the average  $\langle F \rangle$  (by a factor  $\sqrt{cD} \approx 11.4$  in our example), which is also an important characteristic of long-tail distributions.

We now focus on the properties of a  $q$ -HS defined as the region from which a proportion  $q$  of the total SERS signal originates. To determine its relative area  $a_q$ , we first find  $F_q$ , smallest enhancement in the  $q$ -HS (at its edge). It can be obtained from the condition:

$$\int_{F_q}^{F_{\max}} F p(F) dF = q \langle F \rangle, \quad (\text{A10})$$

which leads to

$$F_q = (1-q)^{\frac{1}{1-k}} F_{\max}. \quad (\text{A11})$$

Because the center of the  $q$ -HS corresponds to the place of maximum enhancement, and because the enhancements decay monotonically away from the center of the HS, one can see that  $a_q$  is then simply obtained from:

$$a_q = \int_{F_q}^{F_{\max}} p(F) dF = \frac{AF_{\max}^{-k}}{k} \left[ (1-q)^{-\frac{k}{1-k}} - 1 \right] \quad (\text{A12})$$

For a HS on a sphere (part of a dimer), we can also deduce the half-angle  $\theta_q$  defining a  $q$ -HS:

$$\theta_q = \cos^{-1}(2a_q - 1) \quad (\text{A13})$$

\* Electronic address: Eric.LeRu@vuw.ac.nz

† Electronic address: Pablo.Etchegoin@vuw.ac.nz

<sup>1</sup> S. Nie and S. R. Emory, *Science* **275**, 1102 (1997).

<sup>2</sup> K. Kneipp, Y. Wang, H. Kneipp, L. T. Perelman, I. Itzkan, R. R. Dasari, and M. S. Feld, *Phys. Rev. Lett.* **78**, 1667 (1997).

<sup>3</sup> S. R. Emory, S. Nie, K. Kneipp, and G. R. Harrison, *Chimia* **53**, 35 (1999).

<sup>4</sup> T. O. Shegai and G. Haran, *J. Phys. Chem. B* **110**, 2459 (2006).

<sup>5</sup> A. M. Michaels, M. Nirmal, and L. E. Brus, *J. Am. Chem. Soc.* **121**, 9932 (1999).

<sup>6</sup> A. M. Michaels, J. Jiang, and L. E. Brus, *J. Phys. Chem. B* **104**, 11965 (2000).

<sup>7</sup> H. Xu, J. Aizpurua, M. Käll, and P. Apell, *Phys. Rev. E* **62**, 4318 (2000).

<sup>8</sup> M. Futamata, *Faraday Discussions* **132**, 45 (2006).

<sup>9</sup> E. C. Le Ru and P. G. Etchegoin, *Chem. Phys. Lett.* **396**, 393 (2004).

<sup>10</sup> F. Svedberg and M. Käll, *Faraday Discussions* **132**, 35 (2006), and references therein.

<sup>11</sup> C. J. L. Constantino, T. Lemma, P. A. Antunes, and R. Aroca, *Anal. Chem.* **73**, 3674 (2001).

<sup>12</sup> E. C. Le Ru, M. Meyer, and P. G. Etchegoin, *J. Phys. Chem. B* **110**, 1944 (2006).

<sup>13</sup> E. C. Le Ru, C. Galloway, and P. G. Etchegoin, *Phys. Chem. Chem. Phys.* **8**, 3083 (2006).

<sup>14</sup> P. G. Etchegoin, C. Galloway, and E. C. Le Ru, *Phys. Chem. Chem. Phys.* **8**, 2624 (2006).

<sup>15</sup> J. M. Gérardy and M. Ausloos, *Phys. Rev. B* **25**, 4204 (1982).

<sup>16</sup> O. C. Zienkiewicz and J. Z. Zhu, *Int. J. Numer. Methods Eng.* **32**, 783 (1991).

<sup>17</sup> Sz. Gyimothy and I. Sebestyen, *Applied Electromagnetics and Computational Technology*, edited by H. Tsuboi and I. Sebestyen (IOS Press, Amsterdam, 1997).

<sup>18</sup> O. C. Zienkiewicz and R. L. Taylor, *The Finite Element Method, Vol 1* (McGraw-Hill, New York, 1989), p. 436.

- <sup>19</sup> E. M. Purcell and C. R. Pennypacker, *The Astrophysical Journal* **186**, 705 (1973).
- <sup>20</sup> W. H. Yang, G. C. Schatz, and R. P. van Duyne, *J. Chem. Phys.* **103**, 869 (1995).
- <sup>21</sup> J. J. Goodman, B. T. Draine, and P. J. Flatau, *Opt. Lett.* **16**, 1198 (1991).
- <sup>22</sup> V. A. Markel, L. S. Muratov, M. I. Stockman, and T. F. George, *Phys. Rev. B* **43**, 8183 (1991).
- <sup>23</sup> P. G. Etchegoin and E. C. Le Ru, *J. Phys.: Cond. Mat.* **18**, 1175 (2006).
- <sup>24</sup> E. C. Le Ru and P. G. Etchegoin, *Chem. Phys. Lett.* **423**, 63 (2006).
- <sup>25</sup> R. Rojas and F. Claro, *J. Chem. Phys.* **98**, 998 (1993).
- <sup>26</sup> A. Otto, *Physica Status Solidi A* **188**, 1455 (2001), and references therein.
- <sup>27</sup> E. W. Weisstein, *The Pareto Distribution* (<http://mathworld.wolfram.com/ParetoDistribution.html>)
- <sup>28</sup> The Pareto distribution is associated with the “Pareto principle”, which states that 20% of a population owns 80% of the wealth.
- <sup>29</sup> Z. Zhou, G. Wang, and Z. Xu, *Appl. Phys. Lett.* **88**, 034104 (2006).
- <sup>30</sup> C. C. Neacsu, J. Dreyer, N. Behr, and M. B. Raschke, *Phys. Rev. B* **73**, 193406 (2006).
- <sup>31</sup> H. Xu and M. Käll, *Phys. Rev. Lett.* **89**, 246802 (2002).
- <sup>32</sup> K. Kneipp, Y. Wang, H. Kneipp, I. Itzkan, R. R. Dasari, and M. S. Feld, *Phys. Rev. Lett.* **76**, 2444 (1996).
- <sup>33</sup> A. G. Brolo, A. C. Sanderson, and A. P. Smith, *Phys. Rev. B* **69**, 045424 (2004).
- <sup>34</sup> T. L. Haslett, L. Tay, and M. Moskovits, *J. Chem. Phys.* **113**, 1641 (2000).
- <sup>35</sup> R. C. Maher, L. F. Cohen, E. C. Le Ru, and P. G. Etchegoin, *Faraday Discussions* **132**, 77 (2006).
- <sup>36</sup> R. C. Maher, L. F. Cohen, J. C. Gallop, E. C. Le Ru, and P. G. Etchegoin, *J. Phys. Chem. B* **110**, 6797 (2006).
- <sup>37</sup> R. C. Maher, P. G. Etchegoin, E. C. Le Ru, and L. F. Cohen, *J. Phys. Chem. B* **110**, 11757 (2006).
- <sup>38</sup> R. C. Maher, L. F. Cohen, E. C. Le Ru, and P. G. Etchegoin, *J. Phys. Chem. B* (in press).